Hydration Dynamics near a Model Protein Surface

Daniela Russo[1], Greg Hura[2], Teresa Head-Gordon[1,2,*]
Department of Bioengineering[1] and Graduate Group in Biophysics[2]
University of California, Berkeley CA 94720

The evolution of water dynamics from dilute to very high concentration solutions of a prototypical hydrophobic amino acid with its polar backbone, N-acetyl-leucine-methylamide (NALMA), is studied by quasi-elastic neutron scattering and molecular dynamics simulation for both the completely deuterated and completely hydrogenated leucine monomer. We observe several unexpected features in the dynamics of these biological solutions under ambient conditions. The NALMA dynamics shows evidence of de Gennes narrowing, an indication of coherent long timescale structural relaxation dynamics. The translational water dynamics are analyzed in a first approximation with a jump diffusion model. At the highest solute concentrations, the hydration water dynamics is significantly suppressed and characterized by a long residential time and a slow diffusion coefficient. The analysis of the more dilute concentration solutions takes into account the results of the 2.0M solution as a model of the first hydration shell. Subtracting the first hydration layer based on the 2.0M spectra, the translational diffusion dynamics is still suppressed, although the rotational relaxation time and residential time are converged to bulk-water values. Molecular dynamics analysis shows spatially heterogeneous dynamics at high concentration that becomes homogeneous at more dilute concentrations. We discuss the hydration dynamics results of this model protein system in the context of glassy systems, protein function, and protein-protein interfaces.

*To whom correspondence should be addressed.

Introduction

There is an emerging effort to characterize water and its role as the "twenty-first" amino acid in the broader context of protein folding and function and as mediator for protein-protein interactions(Bellissent-Funel 2000; Bizzarri and Cannistraro 2002; Careri and Peyrard 2001; Dellerue and Bellissent-Funel 2000; Denisov and Halle 1996; Denisov and others 1999; Halle and Denisov 1995; Mattos 2002; Otting 1997; Tarek and Tobias 1999; Tarek and Tobias 2000; Tarek and Tobias 2002; Zanotti and others 1999). In addition to structure and thermodynamics, a wide range of experimental techniques including femto-second spectroscopy(Pal and others 2002), x-ray and neutron scattering(Svergun and others 1998), O^{17} and H^{1} NMR dispersion techniques (Denisov and Halle 1996; Denisov and others 1999; Halle and Denisov 1995; Mattos 2002; Otting 1997), quasi-elastic neutron scattering(Bellissent-Funel 2000; Dellerue and Bellissent-Funel 2000; Diehl and others 1997; Marchi and others 2002; Russo and others 2003a; Zanotti and others 1997; Zanotti and others 1999) and accompanying interpretation and analysis using molecular dynamics (Bizzarri and Cannistraro 2002; Merzel and Smith 2002; Tarek and Tobias 1999; Tarek and Tobias 2000; Tarek and Tobias 2002), have been used to probe hydration dynamics near protein interfaces.

Experimental limitations for studying molecular events in the dynamics of protein water hydration arise from several factors. The highly dilute protein concentrations (required to avoid aggregation) used means that the hydration water dynamics are dominated by bulk water relaxation or diffusion timescales. In other cases the number of hydration waters or other specifics of their hydration sites cannot be directly measured or lack sufficient time-resolution. Furthermore, unlike bulk water, or "crystal" waters that reside in specific locations in the protein interior, study of water dynamics near the protein is limited by the highly averaged information obtained over an inhomogeneous protein surface in various protein conformational states. We note that roughly 50-60% of a folded protein's surface is

hydrophobic(Janin 1999). Thus, it is difficult to distinguish the contribution, for example, arising from a hydrophobic, hydrophilic or aromatic site or between regions more or less exposed to the solvent. Russo et al. have controlled for this protein surface inhomogeneity by characterizing the dynamics of the first interacting water near a completely homogeneous hydrophobic oligopeptide that adopts a beta-sheet conformation (Russo and others 2003a).

In this work we propose a complementary experimental QENS and molecular dynamics simulation study of a greatly simplified protein model system that addresses some of these limitations. We consider the hydration water dynamics near N-acetyl-leucine-methylamide (NALMA), a hydrophobic amino acid side chain attached to a blocked polypeptide backbone, as a function of concentration between 0.5M-2.0M. In previous work we have primarily focused on the structural organization of these peptide solutions and their connection to protein folding (Hura and others 1999; Sorenson and others 1999). Throughout the full concentration range of 0.5M-2.0M studied by x-ray scattering experiments and molecular dynamics simulations, we find that water stabilizes mono-dispersed and small clusters of amino acids, as opposed to more complete segregation of the hydrophobic monomers into a sequestered hydrophobic core(Hura and others 1999; Sorenson and others 1999), which defines the role of water in the later stages of folding. In this work we have performed QENS experiments on both the deuterated and non-deuterated leucine to isolate the hydration water dynamics from the solute motions. Furthermore, two sets of experiments were carried out using different incident neutron wavelengths to give two different time resolutions to separate rotational and translational motion of the hydration dynamics.

The NALMA-water system and the high quality QENS data then provides a unique system for characterizing the dynamics of different hydration layers near a homogeneous hydrophobic amino acid side-chain. By analyzing the diffusion timescales at the highest concentration of 2.0M, where our structural work indicates that NALMA solutes only have

enough water to share one water hydration layer, and comparing it to more dilute concentrations of 0.5M, where each solute has (in principle) enough water for approximately 2-3 hydration layers of its own, permits us to cleanly separate inner sphere and outer sphere hydration dynamics, around a purely hydrophobic amino acid hydration site. We also observe several unexpected features in the dynamics of these biological solutions under ambient conditions. The NALMA dynamics shows evidence of de Gennes narrowing, an indication of coherent long timescale structural relaxation dynamics that are tracked by the self-diffusion measured with QENS. The translational water dynamics of these biological solutions under ambient conditions are analyzed in a first approximation with a jump diffusion model. At the highest solute concentrations, the hydration water dynamics is significantly suppressed and characterized by a long residential time and a slow diffusion coefficient, similar to supercooled water at –10ºC. The analysis of the more dilute concentration solutions has been performed taking in account the results of the 2.0M solution as a model of the first hydration shell. Subtracting the first hydration layer based on the 2.0M spectra, the translational diffusion dynamics is still suppressed, although the rotational relaxation time and residential times are converged to bulk-water values.

The clean separation of rotational and translational timescales allows us to define an experimental "elastic incoherent structure factor" (EISF) from the rotational motion, which can be interpreted as a measure of the fraction of "*immobile*" or localized hydrogen rotational dynamics that are faster or slower than our experimental resolution of 1.0-5.5ps (Bellissentfunel and others 1992; Zanotti and others 1997). The EISF shows significant evolution between 0.5M-2.0M; the EISF for the 0.5M solution measures 37% of immobile hydrogens, whereas only 17% of the protons are not observed for the 2.0M concentrations. The EISF results are supported by MD simulations, in which the lowest concentration shows a presence of long rotational relaxation times near both the hydrophilic and hydrophobic side

chains, while the highest concentration shows more water protons near the hydrophobic side chain whose dynamics become faster, and therefore resolvable by the QENS experiment. The MD results also measure first layer water residence times near hydrophobic and hydrophilic sites, which are spatially heterogeneous at the highest concentrations and which become spatially homogeneous at more dilute concentrations.

This study of the NALMA water solution, and future work that will analyze dynamics near homogeneous hydrophilic and aromatic amino acid monomers, provides an important dissection of hydration dynamics near inhomogeneous protein surfaces. We discuss the implications of the dynamics measured on our model system and its possible connection to supercooled liquids(Angell 1995; Ediger and others 1996; Green and others 1994), protein function(Barron and others 1997; Bellissent-Funel 2000; Bizzarri and Cannistraro 2002; Bu and others 2000; Denisov and others 1999; Tournier and others 2003), and protein-protein interfaces(Bizzarri and Cannistraro 2002).

Experimental Procedures

The main contribution to the scattering cross section of the solution is the incoherent scattering from the protons, and therefore we can isolate the dynamics of the water in the presence of a hydrophobic amino acid by using a completely deuterated leucine solute. The incoherent quasi-elastic CD_3 methyl contributions (30.75 barns) will be considered negligible with respect to one molecule of water contribution (160.4 barns), especially given the large atomic fraction difference between solute and water. The completely deuterated N-acetyl(d_3)-leucine(d_{10})-methylamide(d_3) (MW 202.25) was purchased from CDN Isotopes, Canada. The solution samples were obtained by dissolution of the completely deuterated amino acid powder in pure H_2O at the following concentrations: 0.5M, 1M, 2.0M and 2.3M. In order to

remove aggregated or non-dissolved powder from the solution, each sample was centrifuged (10 min at 10,000 g) before measurement.

The quasi-elastic neutron scattering (QENS) experiment was performed at NIST Center for Neutron Research, using the disk chopper time of flight spectrometer (DCS). In order to separate the translational and rotational components in the spectra, two sets of experiments were carried out using different incident neutron wavelengths of 7.5Å and 5.5Å to give two different time resolutions. The DCS spectrometer operating at the high resolution range of λ=7.5Å with an incident energy of E_{inc}=1.45meV, gives a wave vector range of 0.146 $Å^{-1}$< Q <1.574$Å^{-1}$ and an energy resolution of 35μeV at full width half maximum (FWHM). At the lower resolution, λ=5.5Å and E_{inc}=2.7meV, with the wave vector range covering 0.199$Å^{-1}$ < Q <2.147 $Å^{-1}$ with a FWHM of 81μeV.

The sample containers were two concentric cylinders with radius differing by 0.1mm for the Leu(D): H_2O sample. All the spectra have been measure at room temperature, and the data collection lasted for about 6-10 hours depending on the resolution and sample. The spectra were corrected for the sample holder contribution and normalized using the vanadium standard. The resulting data were analyzed with DAVE programs (http://www.ncnr.nist.gov/dave/). The data has been corrected for the buffer contribution, and we neglect the contribution from the structure factor in the analysis of the spectra.

Experimental Analysis

The experimental quantity measured during a quasi-elastic neutron experiment is the differential cross section, defined as the number of neutrons with a transfer energy dE, scattered into a solid angle dΩ (Bee 1988). The incoherent differential cross section can be experimentally determined as:

$$\frac{d^2\sigma}{dEd\Omega} = \frac{\sigma_{inc}}{4\pi}\frac{k_s}{k_i} NS_{inc}(Q,\omega) \quad (1)$$

where σ is the total incoherent cross section, k_i and k_s are the wavevector of the incident and scattered neutron, Q is the momentum transfer, ω is the frequency, and $S_{inc}(Q,\omega)$ is the incoherent dynamics structure factor. The fit to the experimental data generated at all resolutions used a combination of Lorentzian functions convoluted with the instrumental resolution. The success of the proposed experimental analysis procedure for the hydration dynamics lies in performing two identical experiments corresponding to two different resolutions. The high resolution spectra better characterizes motion arising from translational water diffusion. In the other set of lower-resolution experiments, both translational and rotational contributions are significant. However, since the width of the sharp Lorentzian due to translation is previously determined with accuracy as a function of Q, it is introduced in the Lorentzian fit, favoring the evaluation of the other (rotational) parameters. The compatibility of the low-resolution fit with the high-resolution spectra is then cross-checked, and found to be consistent in our work. Based on those fits we were able to further interpret the data using the following analytical models traditionally applied to liquids (Bee 2003).

$S_{inc}(Q,\omega)$ can be express as a convolution of three terms:

$$S_{inc}(Q,\omega) = e^{-1/3Q^2\langle u^2\rangle} S_{inc}^{trans}(Q,\omega) \otimes S_{inc}^{rot}(Q,\omega) \quad (2)$$

each of which corresponds to a different kind of proton motion (Bee 1988; Bee 2003). The exponential term is the Debye Waller factor, which represents the vibration in the quasi-elastic region; the $\langle u^2 \rangle$ term is the mean square displacement. The second and third terms are the translational and rotational incoherent dynamics structure factor, respectively.

The translational incoherent dynamics structure factor can be described as:

$$S_{inc}^{trans}(Q,\omega) = \frac{1}{\pi}\frac{\Gamma_{trans}(Q)}{\omega^2 + (\Gamma_{trans}(Q))^2} \quad (3)$$

where Γ_{trans} is the half width at half maximum of a Lorentzian function (Bee 1988). The Lorentzian is modeled by a random jump diffusion model, which considers the residence time τ_0 for one site in a given network before jumping to another site (Egelstaff 1992). In this case, the half width at half maximum of the Lorentzian in Eq. (3), will be described as

$$\Gamma^{J}_{trans}(Q) = \frac{D_{trans}Q^2}{1 + D_{trans}Q^2\tau_0} \tag{4}$$

where the mean jump diffusion length L is defined in this model as $L=\sqrt{6D_{trans}\tau_0}$, and D_{trans} is the translational diffusion coefficient between two sites.

The simplest model of internal rotational motion of a molecule corresponds to a random motion of protons on the surface of a sphere (Sears 1966). The rotational incoherent dynamics structure factor is:

$$S_{rot}(Q,\omega) = j_0^2(Qa)\delta(\omega) + \Sigma(2l+1)j_1^2(Qa)\times\frac{1}{\pi}\frac{l(l+1)D_{rot}}{\omega^2 + (l(l+1)D_{rot})^2} \tag{5}$$

where $j_l(Q)$ is a spherical Bessel function of order l; a is the radius of the sphere; and D_{rot} is the rotational diffusion coefficient. For l=1, which dominants the second term of Eq. (5), the half width at half maximum is $\Gamma_{rot} = 2D_{rot}$, which corresponds to a rotational characteristic time of $\tau_{Rotation} = 1/6D_{rot}$.

The first term in Eq. (5) corresponds to the form factor of the restricted volume explored by the hydrogen atoms, known as the "elastic incoherent structure factor" (EISF). Experimentally, the EISF is by definition defined as $I_{elast}(Q)/[I_{elast}(Q)+I_{quasielast}(Q)]$, where $I_{elast}(Q)$ and $I_{quasielast}(Q)$ are the integrated elastic and quasi-elastic scattering respectively. Based on the clean separation of rotational and translational motion of the hydration dynamics, we can define an experimental EISF which is the elastic term of the rotation development (Russo and others, 2003a), and not the traditional form factor of confined diffusion movement more common for protein QENS.

Theoretical Procedure

Analysis of the QENS experiments for aqueous NALMA solutions were aided by molecular dynamics simulations. Various representative solute configurations: dispersed, small molecular aggregates, and fully clustered as described in (Hura and others 1999). Solute configurations at all concentrations were prepared as a maximally dispersed as described in (Hura and others 1999; Sorenson and others 1999). These configurations were equilibrated for 75ps before any statistics were collected.

The AMBER force field due to Cornell et al.(Cornell and others 1995) and the SPCE water model (Berendsen and others 1987) were used for modelling the NALMA solute and water, respectively. The simulations were carried out at 298K in the NVT-ensemble using velocity Verlet integration, velocity rescaling, with a timestep of 1.5fs. Each simulation was equilibrated for 0.1ns and statistics were gathered over the remaining 0.65ns, sampled every 100fs. Ewald sums were used for calculation of the long-range coulomb forces. κ was set to 6.4/L where L is the length of the simulation box and a total of 2×292 *k*-vectors were used ($|k_{max}|^2$ = 26). Rigid-body dynamics for the water solvent were integrated using RATTLE(Anderson 1983).

For the analysis of the water dynamics in the NALMA aqueous solutions, we performed simulations of a dispersed solute configuration consistent with our structural analysis(Hura and others 1999; Sorenson and others 1999). We used the Einstein relation to derive the translational self-diffusion coefficients from the mean square displacement of water oxygens, and the rotational dynamics using the orientational autocorrelation function:

$$exp\left(-6D_{rot}t\right) = P_2\left(t\right) = \left\langle 0.5\left[3\cos^2\theta\left(t\right) - 1\right]\right\rangle \tag{6}$$

where $\theta(t)$ measures the angle between the dipole vector of the water molecule at times t and 0. To analyze the EISF results, we also evaluated an average residence time of water molecules that maintained a distance of 4.0Å or less from the branching carbon center of the hydrophobic side chain, and within 4.0Å of one of the backbone carboxyl oxygens of the NALMA molecule. We also calculate the rotational dynamics of that subset of water molecules maintaining twice that residence time using Eq. (6).

Results

NALMA Solution Structure

Recent x-ray diffraction experiments on aqueous solutions of NALMA performed by our research group(Hura and others 1999; Sorenson and others 1999) has shown that as the solute concentration increases the main diffraction peak of pure water shifts to a smaller Q-value and a new diffraction peak appears at Q=0.8Å^{-1} (Figure 1a). The unaltered Q-value of the new peak position at the higher concentrations suggests that a stable and ordered leucine solute-solute distribution is sustained. Simulations of the spatial distribution of leucine in water at the matched experimental concentrations reproduce the experimental intensity profile (Figure 1b), and when analyzed show that water stabilizes maximally dispersed to small molecular aggregates of hydrophobic amino acids, as opposed to complete segregation of the hydrophobic solutes into one large cluster(Hura and others 1999; Sorenson and others 1999). This supports our hypothesis that a collapsed but water impregnated core could well be transferable into the context of late stages of folding of polypeptide chains(Sorenson and others 1999). The observation of water impregnation late in folding, and the requirement of overcoming a desolvation barrier to reach the native state, has been observed in a large number of simulations(Cheung and others 2002), including the refolding of a beta-hairpin

fragment of protein G(Pande and Rokhsar 1999), and all-atom simulations of protein G(Sheinerman and Brooks 1998), and src-SH3(Shea and others 2002).

Most recently a small angle neutron scattering experiment covering a *Q*-range between 0.008Å^{-1} and 0.3Å^{-1} using the small angle spectrometer PAXE (Orphee', Fr) was performed for NALMA in water over the same range of concentration. The log of the intensity of scattering (absolute units) as a function of the momentum transfer squared Q^2 (Guinier plot) for different concentrations is represented in Figure 2. The Guinier plot shows no appreciable slope at the lower concentrations of 0.5M and 1.0M, while for concentrations of 1.5M and 2.0M the Guinier plot shows a small slope consistent with the small size of a NALMA solute, and excluding the presence of NALMA aggregates formation(Teixeira 2003). Together the wide angle and small angle diffraction measurements provide the structural information complementary to analyze the QENS measurements of hydration and solute dynamics observed over the concentration range studied.

Hydration water dynamics

In order to characterize the perturbation to water dynamics due to the presence of the NALMA solute at various concentrations, the scattering profile of the completely deuterated solute in H_2O has been measured at both high and low resolutions, which allows us to separately resolve the rotational and translational dynamics. The compatibly of the fit for the two resolutions have been cross checked against each other. Figure 3 shows the dynamics incoherent structure factor spectrum, summed over all mean *Q*, measured at 35 μeV and at 81 μeV, for 0.5M and 2.0M NALMA concentration in H_2O. The spectra are normalized to the maximum of the resolution function.

High resolution experiment

The fit to the data generated at high resolution, which probes the slower components of hydration dynamics, required two Lorentzians. The narrow Lorentzian function describes the translational motion, while the broader Lorentzian describes faster movements that will be analyzed simultaneously with the low-resolution data. The translational dynamics is best described by a jump diffusion model based on the dependence of the narrow $\Gamma_{trans}(Q)$ with Q^2 (Figure 4) at all solute concentrations. The resulting diffusion coefficient, D_{trans}, and residential time τ_0 obtained for each concentration are reported in Table I. It is evident that by increasing the NALMA concentration, the $\Gamma_{trans}(Q)$ exhibits an increasingly pronounced plateau at high Q-values, which translates to a longer residential time, while at the smallest Q-values the marginal slope reflects a smaller diffusion coefficient value. At the higher NALMA concentrations the dynamics are substantially suppressed, approaching values more typical of a supercooled water diffusion coefficient and corresponding long residential time. The corresponding molecular dynamics simulation quantities of D_{trans} are in qualitative agreement with experiment over the entire concentration range studied (Table I).

Given the evidence that the solution structural organization does not change over the concentration range of 0.5M-2.3M, a supplementary analysis can be performed for the lower concentration data. Assuming that the dynamics of the first hydration shell of ~25 waters around the NALMA is completely described by the analysis of the 2.0M data, it may be possible to characterize the dynamical behavior of the outer hydration sphere separately using the 1M data. The analysis is comprised of subtracting the data with the 2.0M translational linewidths as known values, leaving the remaining data to be fit by two free Lorentzian functions. In Figure 5a we show the new Γ_{trans} inferred from this analysis in comparison with the 0.5M and 1M half width obtained with the standard analysis. The new translational dynamics for 1.0M is quite similar to the 0.5M hydration water dynamics, with a translational diffusion coefficient of the same order of magnitude but with a longer residential time. In

Figure 5b we show the reanalyzed 0.5M data by taking into account the results of the 2.0M data, exactly in the manner in which we reanalyzed the 1.0M data. Together the 0.5M and 1.0M data results show that the translational dynamics of the outer sphere hydration layer(s) of water are in themselves perturbed from bulk-like water dynamics.

Correlating the linewidth of the broader Lorentzian and its intensity dependence on Q, together with the intensity of the narrow Lorentzian, we attribute the large linewidths as arising from hydrogen rotation. For the 2.0M data, Γ_{rot} is clearly independent of Q and shows small error. The Γ_{rot} is 0.1meV for these highest concentrations, which corresponds to a rotational relaxation time of about 2.2ps, longer than that of bulk water and consistent with the suppressed translational dynamics seen for the high concentration solutions. However, the linewidth of the broader Lorentzian for the 1.0M and 0.5M data gives a larger error in the fit to the intensity data, which therefore will be better analyzed with the low-resolution data.

Low resolution experiment

The data from the low-resolution runs were analyzed by including the narrow translational Lorentzian functions based on the high-resolution experiment as known values. The remaining motion is due to rotation, and we plot the resulting Γ_{rot} as a function of concentration in Figure 6. The characteristic Γ_{rot} of the hydration water at 2.0M and 2.3M measured at low-resolution shows the proper lack of Q-dependence with an average value equal to 0.1meV, a value that is consistent with the high-resolution analysis (Table I). In this particular case, the best fit has been obtained by including a third Lorentzian function, the $l=2$ term in Eq.(5); only when the data is of high quality can we resolve terms where $l>1$.

Next we turn to the analysis of the low concentration data. At 1.0M and 0.5M, the data was first analyzed by fitting the spectra with two Lorentzians. However, the inferred Γ_{rot}

appears to increase for Q^2>2.0, suggesting that a small translational component is present in the low-resolution data. In this case we introduce a third Lorentzian function, corresponding to the 2.0M translational water dynamics, as a model of the first hydration shell at more dilute NALMA concentrations. Once the translational dynamics of the first hydration layer is subtracted, the remaining signal gives a broad linewidth that is independent of Q, with a mean value of 0.22.0MeV for both the 1.0M and 0.5M data, which corresponds to a characteristic rotational relaxation time of 1ps (Table I). The intensity modeled in this way correctly gives translation and rotation functions that follow $j_0(Qa)$ and $j_1(Qa)$ behavior, respectively, while the intensity of the third Lorentzian is independent of Q with small amplitude. Again we see that molecular dynamics estimates of rotational dynamics quantitatively support the experimental values obtained over the full concentration range (Table I).

Figure 7 presents the hydration water EISF variation as a function of NALMA concentration. It is possible to estimate from the experimental EISF the number of "*immobile*" or localized hydrogen rotational dynamics, i.e. hydrogen motions that are faster or slower than the experimental resolution(Bellissentfunel and others 1992; Zanotti and others 1997). In this experiment, the EISF is the elastic term of the rotational motion in Eq. (5), for which we only observe rotational motions on timescales between 1-5.5ps. For the total intensity we do not take into account intensity arising from the translational motion analyzed from the 2.0M contribution to the 1M and 0.5M spectrum. The EISF shows a significant evolution between the 0.5M and the 2.0M concentrations. At 0.5M the percentage of *immobile* hydrogen is 37%, which is much higher than the 17% observed at 2.0M.

This seemingly puzzling result was analyzed by molecular dynamics simulation, in which the rotational relaxation times and residence times of water molecules were monitored at two different sites near the NALMA solute (see Methods and Table II). We find that at

0.5M the residence times are largely equal near both sites: ~8.5-9.0ps; however at 2.0M we find that the residence times are very different between the two sites: ~3.5-4.0ps near the hydrophobic side chain, whereas it is ~10.0-10.5ps near the hydrophilic site (Table II). For 0.5M there are ~325 water molecules with the average residence time or longer (over the length of the 2.15ns simulation), whereas for 2.0M there are only ~110 water molecules with the average residence time, with the greatest depletion in slow waters absenting themselves from the hydrophobic site (Table II). The orientational autocorrelation $P_2(t)$ function of water molecules with these average residence times or longer, for each site and each concentration, are shown in Figure 8. The 0.5M $P_2(t)$ data are well fit with two exponentials, and show populations with very slow rotational timescales (~6-8 ps) and fast rotational timescales (~1 ps). The 2.0M $P_2(t)$ data is best fit with one exponential, with a slow rotational timescales (~4-5ps) near the hydrophilic site, and faster rotational timescales (~2 ps) near the hydrophobic site. A stretched exponential model, $\exp(-t/\tau)^{\beta}$, also provided a good fit to the autocorrelation function of the 2M data as well as the 0.5M data, with a β–exponent value between 0.4-0.6. This complementary analysis confirms that the over the full range NALMA concentration that there is a distribution of rotational time scales.

In the end there are more waters outside the resolution range of the QENS experiment for the 0.5M concentration, while at higher concentrations we observe faster water motions near the hydrophobic side chain that come back into the experimental resolution window. Qualitatively we attribute the higher percentage of localized hydrogens seen at 0.5M as arising from the better ability to form more idealized hydrogen-bonded networks around the hydrophobic side chain. By contrast the reduced levels of immobile hydrogens at higher NALMA concentrations results in a more strained-non-optimal network that breaks more easily to permit faster motions.

NALMA (leucine) dynamics

We first analyze the leucine dynamics by fitting the data with one Lorentzian function. The translational linewidth at half width half maximum, $\Gamma(Q)$, is represented in Figure 9a for all concentrations; its dependence on Q follows to a reasonable approximation the hydrodynamic regime behavior, yielding a diffusion coefficient value that ranges between 3.1–3.6x10^{-6} cm^2/s, and therefore roughly constant over the full concentration range (Table I). In the observed dynamical range of the experiment only the random walk is observed, and to isolate the side chain movement from the Brownian diffusion another instrumental resolution would be needed. From the diffusion coefficient, measured at the lowest concentration, a value of 6Å has been extracted for the hydrodynamic radius. Molecular dynamics simulations show quantitative agreement in the evaluated NALMA translational diffusion constants at the lowest concentration but deviates from the experimental 2.0 M data. (Table I).

In Figure 9b we plot the integrated intensity over energy as a function of Q and concentration; the integrated intensity exhibits a characteristic broad peak at ~0.8$Å^{-1}$, consistent with the x-ray diffraction data. Because our analysis of the integrated intensity shows that the peak cannot be isolated from an elastic component, it suggests that a collective dynamical component is present. In the same figure, we plot $\Gamma(Q)*Q^2$ versus Q, in which we observe a deviation from the expected independence of Q, and showing a corresponding weak minimum in $\Gamma(Q)*Q^2$ at the same wave vector as the maximum in the integrated intensity. Thus the NALMA dynamics are consistent with “de Gennes narrowing” (de Gennes, 1959), which can be narrowly interpreted as NALMA self-diffusion from the incoherent dynamics which tracks the coherent dynamics of the collective motion. An alternative viewpoint is that the observed de Gennes narrowing effect is an indicator of long timescale structural relaxation of water-caged leucine solutes. We will investigate this coherent contribution in future work.

Given the presence of the coherent dynamics contribution to the leucine dynamics spectra, and the simulated self-diffusion coefficient of $1.0x10^{-6}$ cm^2/s, a different analysis strategy has been used. The analysis has been performed by fitting the data with three Lorentzian functions, without subtracting the aqueous D_2O background. We impose the $\Gamma_{trans}(Q)$ consistent with the MD simulation, and we leave the remaining Lorentzians free to fit the remaining buffer contribution and possibly the coherent contribution, presented in Figure 9c. The detected buffer dynamics contribution is in excellent accord to our previous hydration water dynamics results for the 2M deuterated NALMA (Figure 4), while the second free Lorentzian is very broad and present two minimum at ~$0.8Å^{-1}$ and ~$1.1Å^{-1}$. The HWHM of the second Lorentzian is very broad and to noisy, and is only an alternative analysis, and is the most that we can extrapolate from this data.

An important corollary that emerges from the integrated QENS intensity, which exploits scattering contrast to isolate the NALMA correlations, is further support that the structural organization of the leucines in solution is identical over the full concentration range from 0.5-2.0M, something that was not fully resolvable by diffraction at the lower concentrations. This implies that at 0.5M and 1.0M, the NALMA organizes into water-penetrated clusters, and therefore their first hydration layer dynamics can be analyzed in terms of the dynamics of the 2.0M data.

Conclusion

In this work we have considered the hydration water dynamics near a model protein system, N-acetyl-leucine-methylamide (NALMA), a hydrophobic amino acid side chain attached to a blocked polypeptide backbone, as a function of concentration between 0.5M-2.3M. The consistent dynamical picture that emerges is the presence of two proton families contributing to the quasi-elastic signal. One family arises from the slower dynamics

represented by the first water layer that shows "supercooled" diffusional behavior and suppressed rotational motion (i.e. values consistent with bulk water at approximately -10°C). The second component arises from outer layer(s) water dynamics, which exhibits bulk water rotational motion times, and faster translational dynamics than the first hydration layer, but which does not fully recover to room temperature "bulk-like" translational diffusion values. We also find evidence of collective motion of the NALMA solutes that is consistent with de Gennes narrowing, with a self-diffusion constant that is almost an order of magnitude slower than accompanying hydration dynamics.

An additional goal of this work is to precisely study water dynamics as a function of its location in a situation better defined and less complex than a natural biological molecule. We note that a folded protein's surface is roughly equally distributed between hydrophobic and hydrophilic domains, whose lengthscales are on the order of a few water diameters, and which justify our study of hydration dynamics of the simple NALMA system with both hydrophilic and hydrophobic regions. The systematic study of the NALMA water hydration dynamics provides an important dissection of hydration dynamics near inhomogeneous protein surfaces, with implications for supercooled liquids, protein folding and function, and protein-protein interfaces. Given these caveats of our simplified model protein, we provide comment and contrast to hydration dynamics observed near real proteins surfaces.

There is greater uncertainty in the literature about how much the dynamics of outer hydration layers are perturbed by the protein interface, with some studies supporting the view that the outer layer dynamics have recovered bulk-like water dynamics, while other analysis suggest perturbations well into the second or third layer. Recent work has supported the provocative suggestion that outer layer dynamics are up to *50 times slower* than inner protein layer dynamics, and might support "slip streams" for ligand or metabolite diffusion to relevant protein active sites. Our results find faster water diffusion in outer hydration layers

relative to the first hydration level, but still suppressed with respect to bulk-like values, whereas rotational motions in outer layers are fully recovered to bulk water values.

We also find qualitatively different hydration dynamics at low and high concentrations near the model protein hydrophobic and hydrophilic sites. This spatial heterogeneity in the dynamics at low hydration becomes spatially homogeneous at higher hydration levels of our model protein system. These results also allow us to provide a hypothesis for the molecular mechanism of the solvent motion that is required to trigger protein structural relaxation and the onset of protein function when above a critical hydration level(Russo and others 2003b). We hypothesize that below the critical hydration level, water dynamics near hydrophobic sites is much faster and incommensurate with that near the hydrophilic sites; it is *too fast* to effectively solvate the hydrophobic side chains, and the hydrogen-bonded water network is dynamically unstable. At a sufficient level of hydration, the hydration dynamics become spatially homogeneous, with restoration of a water network that can support hydrophobic hydration over sufficient time scales that are *slow* enough to couple to protein conformational transitions to realize the structural plasticity necessary for protein function.

Due to the high density of molecules within the cell, there can on average only be two to three hydration layers between proteins (Mentre, 1995). We do see spatially heterogeneous dynamics at low hydration levels that might have functional importance in the crowded cell or at a protein-protein interface. Perhaps analysis of hydrophilic and hydrophobic patterns on protein surfaces should be analyzed for “slip streams” into active sites (our results suggesting that one follow hydrophobic tributaries), or for protein-protein molecular recognition events involving arrested water motions to aid docking.

Acknowledgments

We gratefully acknowledge the support of NIH GM65239-01. This work utilized facilities supported in part by the National Science Foundation under Agreement No. DMR-0086210. We acknowledge the support of the National Institute of Standards and Technology, U.S. Department of Commerce, in providing the neutron research facilities used in this work. The authors acknowledge Dr. John Copley for assisting on the DCS spectrometer and thank Dr. Jose' Teixeira for performing the small angle neutron experiment on the PAXE spectrometer.

References

Anderson HC. 1983. Rattle: a "velocity" version of the shake algorithm for molecular dynamics calculations. J. Comp. Phys. 52:24-34.

Angell CA. 1995. FORMATION OF GLASSES FROM LIQUIDS AND BIOPOLYMERS [Review]. Science 267(5206):1924-1935.

Barron LD, Hecht L, Wilson G. 1997. The Lubricant of Life - a Proposal That Solvent Water Promotes Extremely Fast Conformational Fluctuations in Mobile Heteropolypeptide Structure. Biochemistry 36(43):13143-13147.

Bee M. 1988. Quasi-elastic neutron scattering. Philadelphia: Adam Hilger.

Bee M. 2003. Localized and long-range diffusion in condensed matter: state of the art of QENS studies and future prospects. Chemical Physics 292(2-3):121-141.

Bellissent-Funel MC. 2000. Hydration in protein dynamics and function. Journal of Molecular Liquids 84(1):39-52.

Bellissentfunel MC, Teixeira J, Bradley KF, Chen SH. 1992. Dynamics of hydration water in protein. Journal de Physique I 2:995.

Berendsen HJ, Grigera JR, Straatsma TP. 1987. The missing term in effective pair potentials. J. Phys. Chem. 91:6269-6271.

Bizzarri AR, Cannistraro S. 2002. Molecular dynamics of water at the protein-solvent interface [Review]. Journal of Physical Chemistry B 106(26):6617-6633.

Bu ZM, Neumann DA, Lee SH, Brown CM, Engelman DM, Han CC. 2000. A view of dynamics changes in the molten globule-native folding step by quasielastic neutron scattering. Journal of Molecular Biology 301(2):525-536.

Careri G, Peyrard M. 2001. Physical aspects of the weakly hydrated protein surface [Review]. Cellular & Molecular Biology 47(5):745-756.

Cheung MS, Garcia AE, Onuchic JN. 2002. Protein folding mediated by solvation: Water expulsion and formation of the hydrophobic core occur after the structural collapse. Proceedings of the National Academy of Sciences of the United States of America 99(2):685-690.

Cornell WD, Cieplak P, Bayly CI, Gould IR, Merz KM, Ferguson DM, Spellmeyer DC, Fox T, Caldwell JW, Kollman PA. 1995. A Second Generation Force Field for the Simulation of Proteins, Nucleic Acids, and Organic Molecules. J. Am. Chem. Soc. 117(19):5179-5197.

Dellerue S, Bellissent-Funel MC. 2000. Relaxational dynamics of water molecules at protein surface. Chemical Physics 258(2-3):315-325.

Denisov VP, Halle B. 1996. Protein Hydration Dynamics in Aqueous Solution. Faraday Discussions(103):227-244.

Denisov VP, Jonsson BH, Halle B. 1999. Hydration of denatured and molten globule proteins. Nature Structural Biology 6(3):253-260.

Diehl M, Doster W, Petry W, Schober H. 1997. Water-Coupled Low-Frequency Modes of Myoglobin and Lysozyme Observed by Inelastic Neutron Scattering. Biophysical Journal 73(5):2726-2732.

Ediger MD, Angell CA, Nagel SR. 1996. SUPERCOOLED LIQUIDS AND GLASSES [Review]. Journal of Physical Chemistry 100(31):13200-13212.

Egelstaff PA. 1992. An introduction to the liquid state. Oxford: Clarendon.

Green JL, Fan J, Angell CA. 1994. THE PROTEIN-CLASS ANALOGY - SOME INSIGHTS FROM HOMOPEPTIDE COMPARISONS [Review]. Journal of Physical Chemistry 98(51):13780-13790.

Halle B, Denisov VP. 1995. A New View of Water Dynamics in Immobilized Proteins. Biophysical Journal 69(1):242-249.

Hura G, Sorenson JM, Glaeser RM, Head-Gordon T. 1999. Solution X-ray scattering as a probe of hydration-dependent structuring of aqueous solutions [Review]. Perspectives in Drug Discovery & Design 17(1):97-118.

Janin J. 1999. Wet and dry interfaces: the role of solvent in protein-protein and protein-DNA recognition [Review]. Structure with Folding & Design 7(12):R277-R279.

Marchi M, Sterpone F, Ceccarelli M. 2002. Water rotational relaxation and diffusion in hydrated lysozyme. Journal of the American Chemical Society 124(23):6787-6791.

Mattos C. 2002. Protein-water interactions in a dynamic world [Review]. Trends in Biochemical Sciences 27(4):203-208.

Merzel F, Smith JC. 2002. Is the first hydration shell of lysozyme of higher density than bulk water? Proceedings of the National Academy of Sciences of the United States of America 99(8):5378-5383.

Otting G. 1997. NMR STUDIES OF WATER BOUND TO BIOLOGICAL MOLECULES [Review]. Progress in Nuclear Magnetic Resonance Spectroscopy 31(Part 2-3):259-285.

Pal SK, Peon J, Zewail AH. 2002. Biological water at the protein surface: Dynamical solvation probed directly with femtosecond resolution. Proceedings of the National Academy of Sciences of the United States of America 99(4):1763-1768.

Pande VS, Rokhsar DS. 1999. Molecular dynamics simulations of unfolding and refolding of a beta-hairpin fragment of protein G. Proceedings of the National Academy of Sciences of the United States of America 96(16):9062-9067.

Russo D, Baglioni P, Peroni E, Teixeira J. 2003a. Picosecond hydration water dynamics of a completely hydrophobic small peptide. Chem. Phys. Vol 292/2-3 pp 235-245.

Russo D, Hura G, Head-Gordon T. 2003b. Hydration Water Dynamics and Instigation of Protein Structural Relaxation. JACS Communication submitted.

Sears VF. 1966. Canadian Journal of Physics 44:1299.

Shea JE, Onuchic JN, Brooks CL. 2002. Probing the folding free energy landscape of the src-SH3 protein domain. Proceedings of the National Academy of Sciences of the United States of America 99(25):16064-16068.

Sheinerman FB, Brooks CL. 1998. Molecular Picture of Folding of a Small Alpha/Beta Protein. Proceedings of the National Academy of Sciences of the United States of America 95(4):1562-1567.

Sorenson JM, Hura G, Soper AK, Pertsemlidis A, Head-Gordon T. 1999. Determining the role of hydration forces in protein folding. Journal of Physical Chemistry B 103(26):5413-5426.

Svergun DI, Richard S, Koch MHJ, Sayers Z, Kuprin S, Zaccai G. 1998. Protein Hydration in Solution - Experimental Observation by X-Ray and Neutron Scattering. Proceedings of the National Academy of Sciences of the United States of America 95(5):2267-2272.

Tarek M, Tobias DJ. 1999. Environmental dependence of the dynamics of protein hydration water. Journal of the American Chemical Society 121(41):9740-9741.

Tarek M, Tobias DJ. 2000. The dynamics of protein hydration water: A quantitative comparison of molecular dynamics simulations and neutron-scattering experiments. Biophysical Journal 79(6):3244-3257.

Tarek M, Tobias DJ. 2002. Role of protein-water hydrogen bond dynamics in the protein dynamical transition - art. no. 138101. Physical Review Letters 8813(13):8101.

Teixeira J. 2003.

Tournier AL, Xu JC, Smith JC. 2003. Translational hydration water dynamics drives the protein glass transition. Biophysical Journal 85(3):1871-1875.

Zanotti JM, Bellissentfunel MC, Parello J. 1997. Dynamics of a Globular Protein as Studied by Neutron Scattering and Solid-State Nmr. Physica B 234:228-230.

Zanotti JM, Bellissent-Funel MC, Parello J. 1999. Hydration-coupled dynamics in proteins studied by neutron scattering and NMR: The case of the typical EF-hand calcium-binding parvalbumin. Biophysical Journal 76(5):2390-2411.

Table I. Experimental and simulation values (in parentheses) for NALMA and water dynamics as a function of NALMA concentration. Translational diffusion coefficient, D_{trans} for NALMA and water, the rotation time for water, $\tau_{rotation}$, and the residence time of water based on the jump diffusion model, τ_o.

[NALMA]	**0.5M**	**1M**	**2.0M**
D_{trans} NALMA (10^{-5} cm^2/s)	0.33 (**0.28**)	0.36	0.31 (**0.1**)
D_{trans}Water (10^{-5} cm^2/s)	1.65 (**1.3**)	1.26	0.75 (**0.80**)
$\tau_{rotation}$ (ps)	1.0 (**1.3**)	1.0	2.2 (**2.25**)
τ_o (ps)	0.94	1.9	3.6

Table II. Simulation analysis for water dynamics. The residence time, $\tau_{res,}$ and rotational timescales of water in the first hydration shell near hydrophobic and hydrophilic sites of the NALMA solute. The orientational autocorrelation function for waters with with τ_{res} is fit to the following functional form:

$$A_0\exp(-t/\tau_1)+A_1\exp(-t/\tau_2)+A_2$$

Site	**τ_{res} (ps)**	**Number waters/NALMA with τ_{res}**	**A_0**	**A_1**	**A_2**	**τ_1 (ps)**	**τ_2 (ps)**
	0.5M						
Hydrophilic	8.5-9.0	63	0.40	0.27	0.005	8.2	1.30
Hydrophobic	8.5-9.0	77	0.31	0.35	0.085	6.4	0.88
	2.0M						
Hydrophilic	10.5-11.0	44	0.49	0.0	0.076	4.8	0.0
Hydrophobic	3.5-4.0	10	0.56	0.0	0.033	2.0	0.0

Figure Captions

Figure 1. (a) *X-ray scattering intensity curves for pure water and NALMA in water solutions at concentrations of solute to water of 1:25 and 1:50*. The data has been scaled to the pure water scattering data of Nishikawa and Kitagawa. **(b)** *Simulated X-ray scattering intensity curves for pure water and NALMA in water at concentrations of solute to water of 1:24 and 1:47, with NALMAs maximally dispersed.* The data is calculated on an absolute scale.

Figure 2. The log of the small angle intensity of scattering (absolute units) as a function of the momentum transfer squared Q^2 (Guinier plot) for NALMA in water solutions at solute concentrations of 0.5M, 1M, 1.5M and 2.0M.

Figure 3. The incoherent structure factor spectrum, summed over all mean Q, for 0.5M (dotted line) and 2.0M (dashed line) NALMA concentration in H_2O measured at 35 μeV (top) and 81 μeV (bottom). The spectra are normalized to the maximum of the resolution function, which is represented by the bold line.

Figure 4. Half width at half maximum of the Lorentzian function, $\Gamma_{trans}(Q)$, plotted versus Q^2 for the deuterated NALMA in H_2O at high resolution for 0.5M, 1M and 2.0M NALMA concentration and for bulk water. The solid line is the fit based on the random jump model.

Figure 5. Half width at half maximum, $\Gamma_{trans}(Q)$, of the Lorentzian function plotted versus Q^2 for the deuterated NALMA in H_2O at high resolution for **(a)** 1.0M and **(b)** 0.5M NALMA. The analysis is comprised of subtracting the 2.0M translational linewidths from the low concentration data. By subtracting out the first hydration shell, the new translational dynamics for 1.0M is quite similar to the 0.5M hydration water dynamics, with a translational diffusion coefficient of the same order of magnitude but with a longer residential time.

Figure 6. HWHM of the Lorentzian function, $\Gamma_{rot}(Q)$, plotted versus Q^2, for 0.5M, 1M and 2.0M NALMA concentration, corresponding to the rotational motions of protons, at different solute concentration.

Figure 7. EISF of hydration water plotted versus Q^2, for 0.5M, 1M and 2.0M NALMA concentration.

Figure 8. The orientational autocorrelation function, $P_2(t)$, for waters that maintained a distance of 4.0Å or less from the branching carbon center of the hydrophobic side chain, and within 4.0Å of one of the backbone carboxyl oxygens of the NALMA molecule for at least τ_{res}. The 0.5M $P_2(t)$ data are well fit with two exponentials, and show populations with very slow rotational timescales (~6-8 ps) and fast rotational timescales (~1ps). The total 2.0M $P_2(t)$ data is best fit with one exponential, which arises from a slow rotational timescales (~4-5ps) near the hydrophilic site, and faster rotational timescales (~2 ps) near the hydrophobic site.

Figure 9. (a) Half width at half maximum, $\Gamma_{trans}(Q)$, of the Lorentzian as a function of Q^2, for the hydrogenated NALMA in D_2O at high-resolution. **(b)** Integrated intensities of the Lorentzian functions, plotted versus Q, for 0.5M, 1M and 2.0M NALMA concentration. The spectra are characteristic of a broad peak at $0.85Å^{-1}$, consistent with the x-ray diffraction data in (Hura and others 1999; Sorenson and others 1999), which correspond to a minimum in the $HWHM/Q^2$, in agreement with "de Gennes narrowing" effect. **(c)** Half width at half maximum, HWHM, for analysis with three Lorentzian functions as a function of Q^2, for the 2M hydrogenated NALMA in D_2O, without buffer subtraction. The first Lorentzian is fixed to that corresponding to the simulated D_{trans}, while the remaining two Lorentzians are free. The second Lorentzian represents the water dynamics, and is in excellent agreement with the data presented in Figure 4. The remaining Lorentzian is a broad component that seems to exhibit the behaviour of the coherent contribution.

(a)

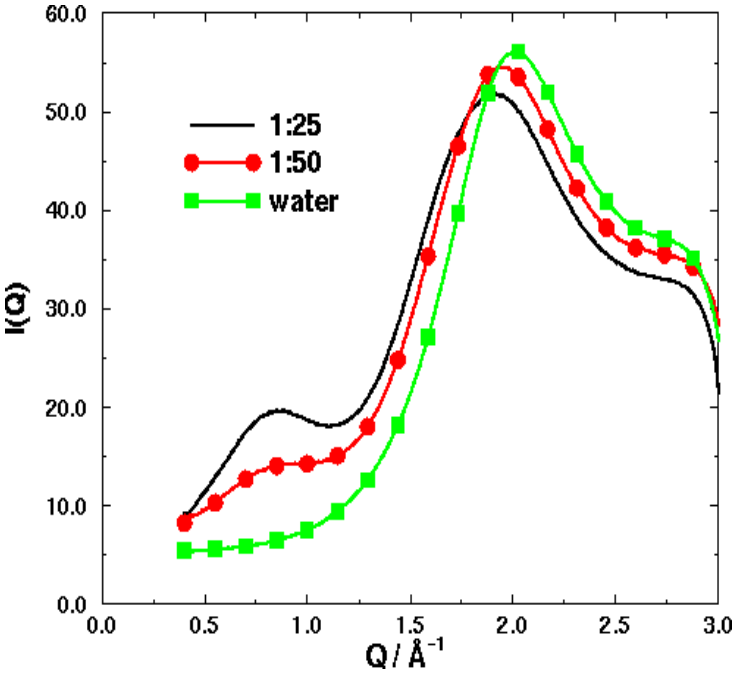

(b)

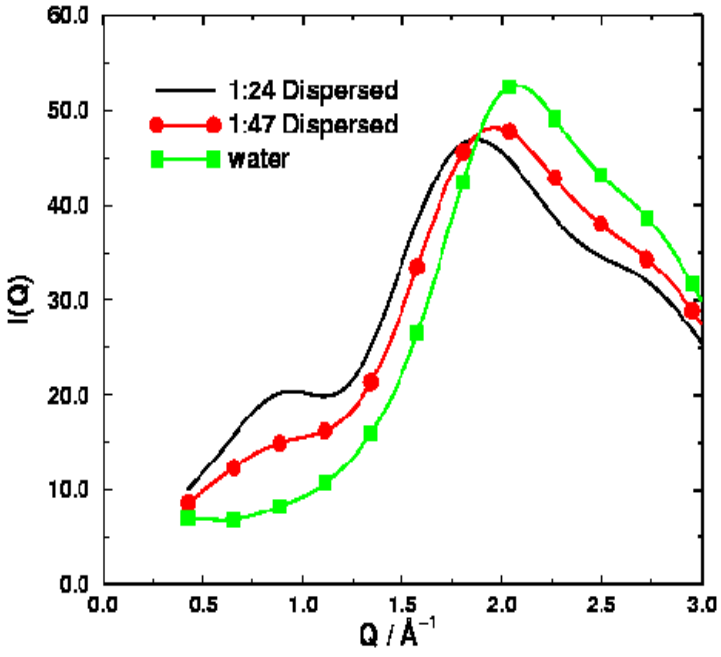

Figure 1. Russo et al.

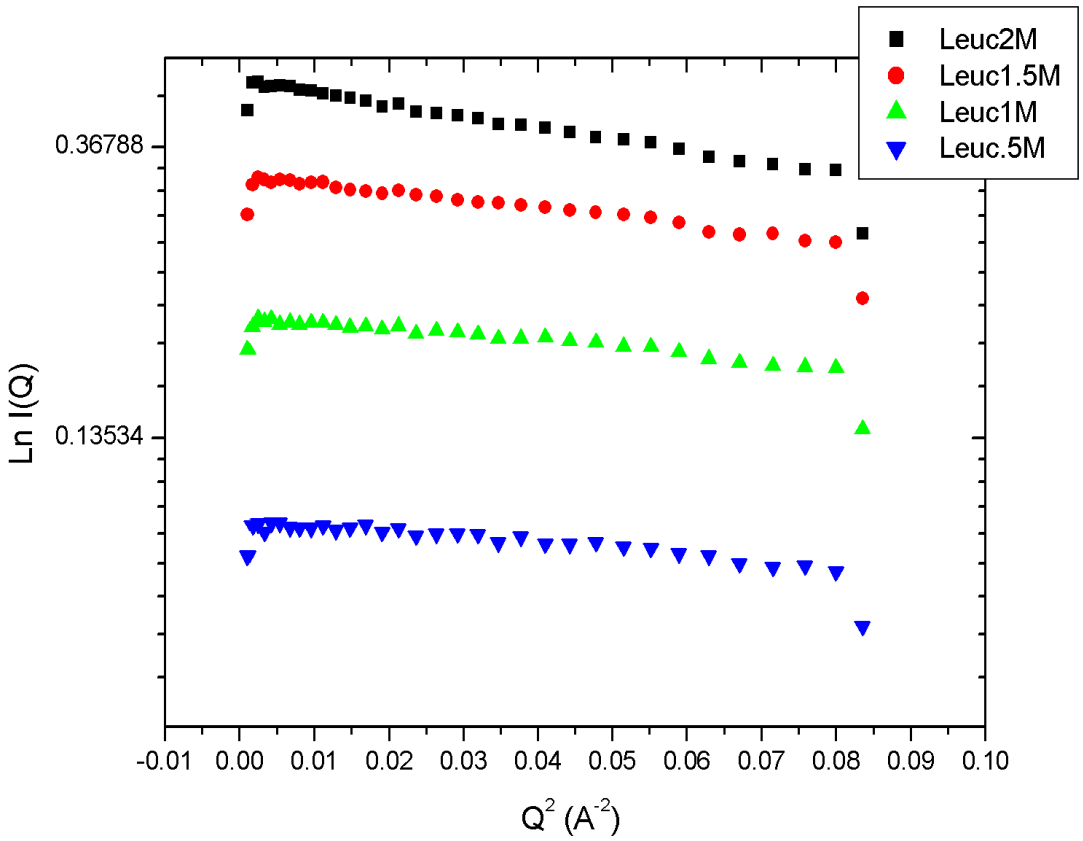

Figure 2. Russo et al.

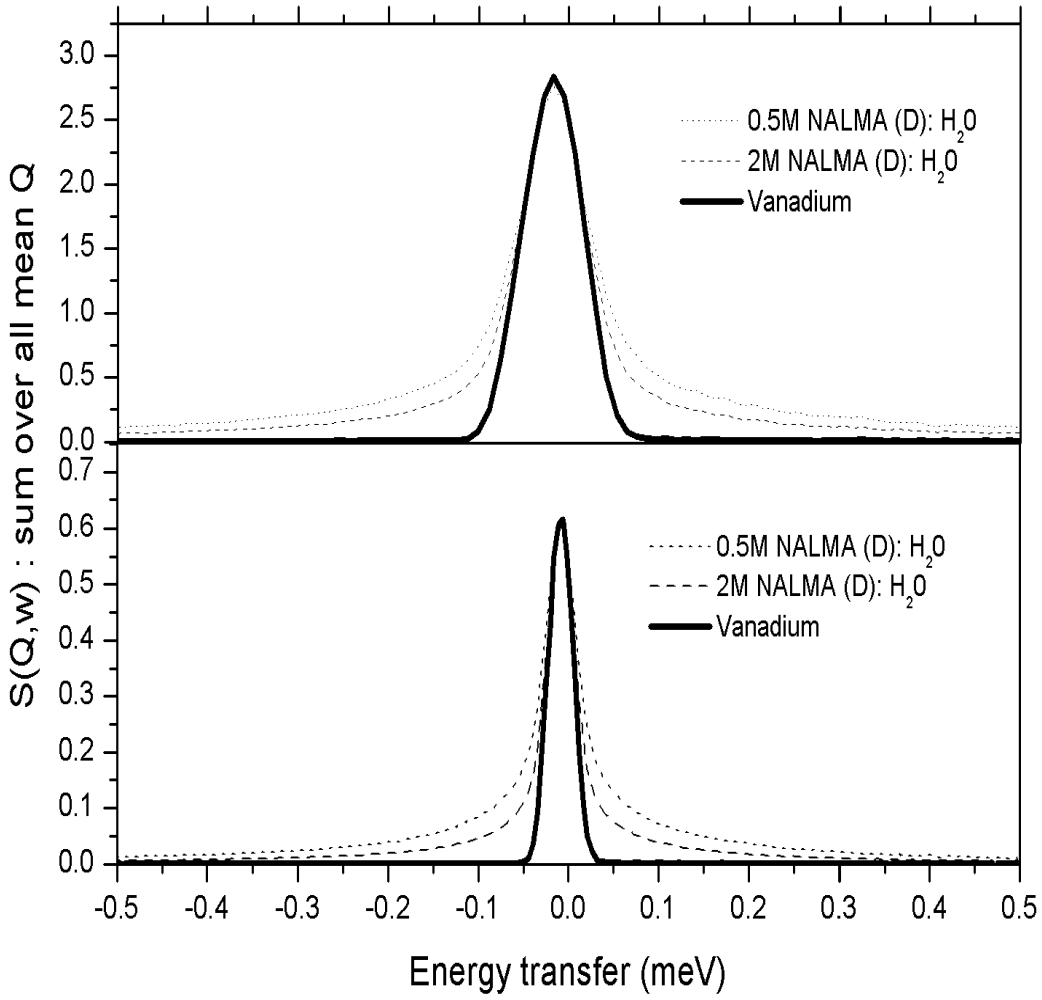

Figure 3. Russo et al.

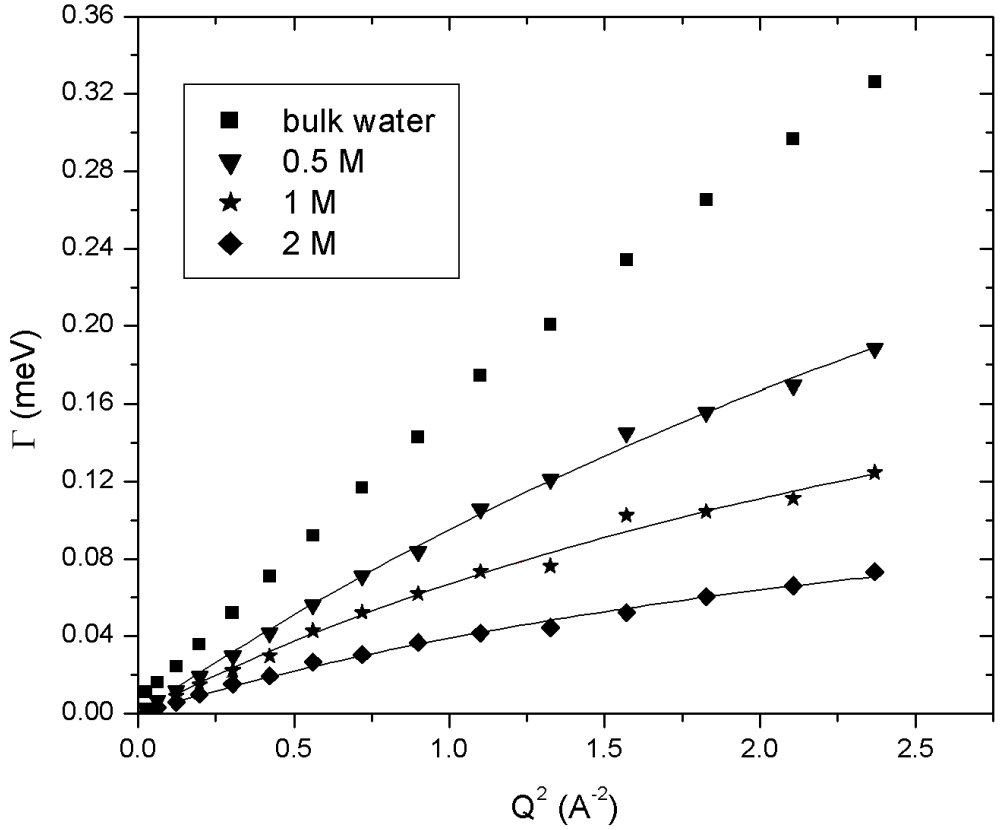

Figure 4. Russo et al.

(a)

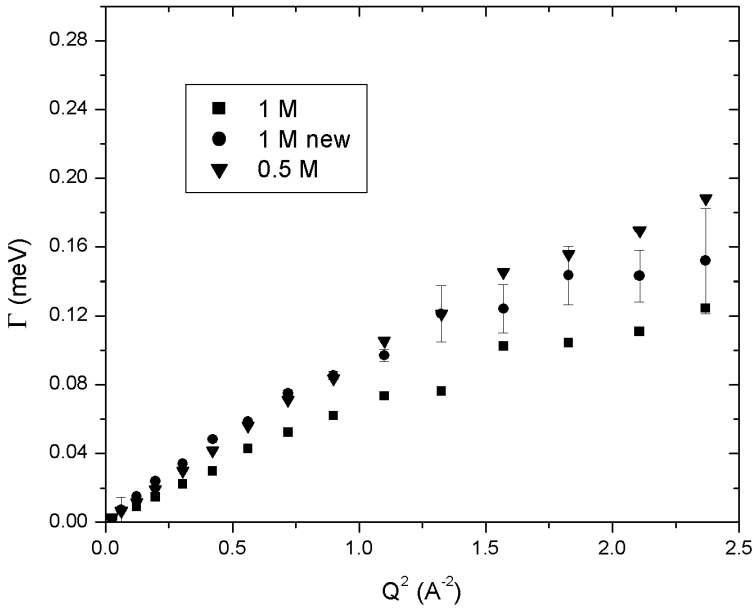

(b)

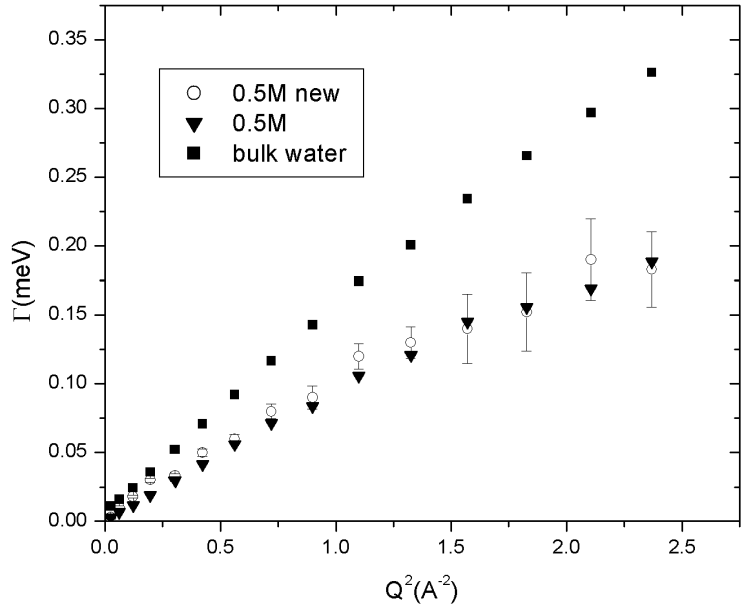

Figure 5. Russo et al.

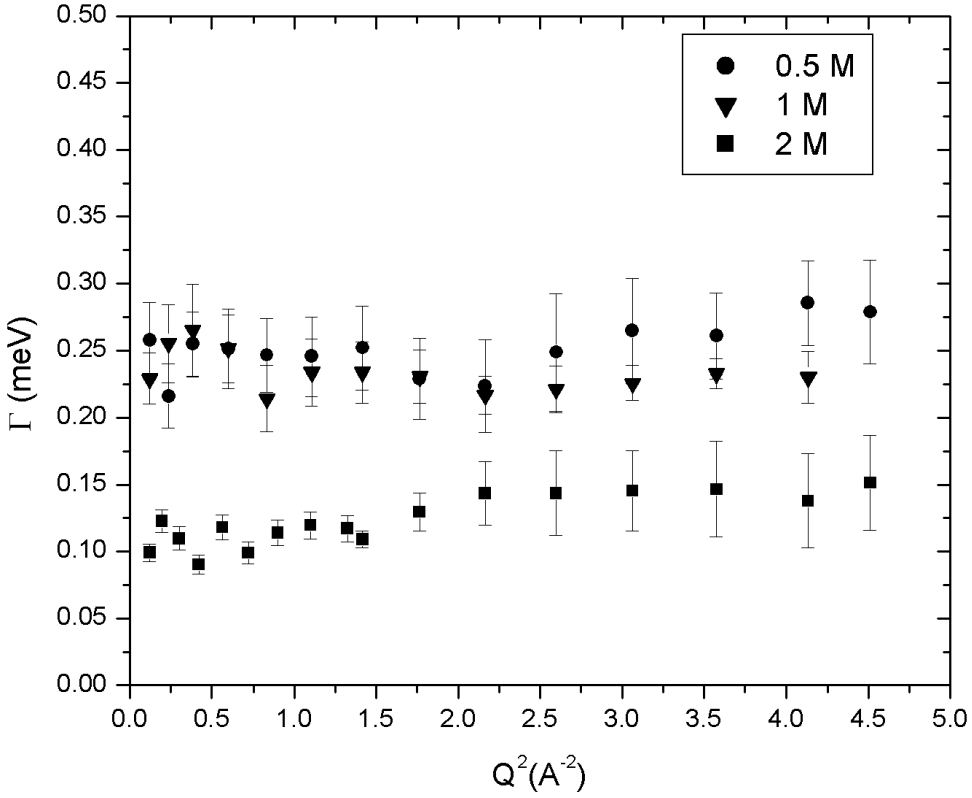

Figure 6. Russo et al.

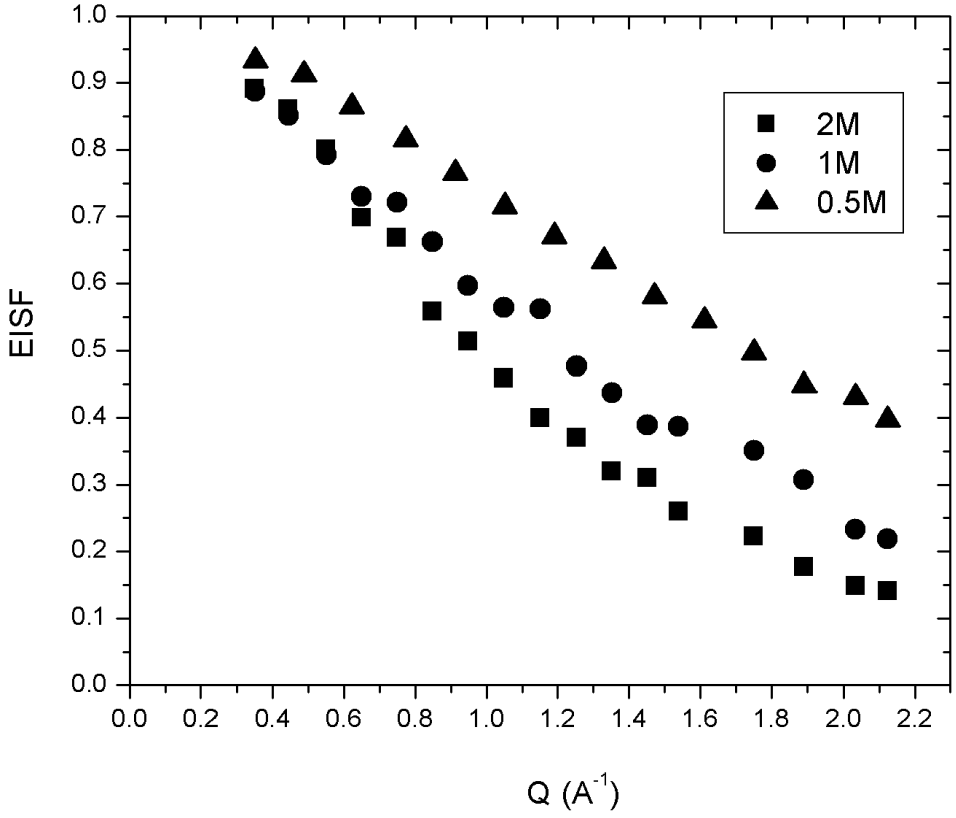

Figure 7. Russo et al.

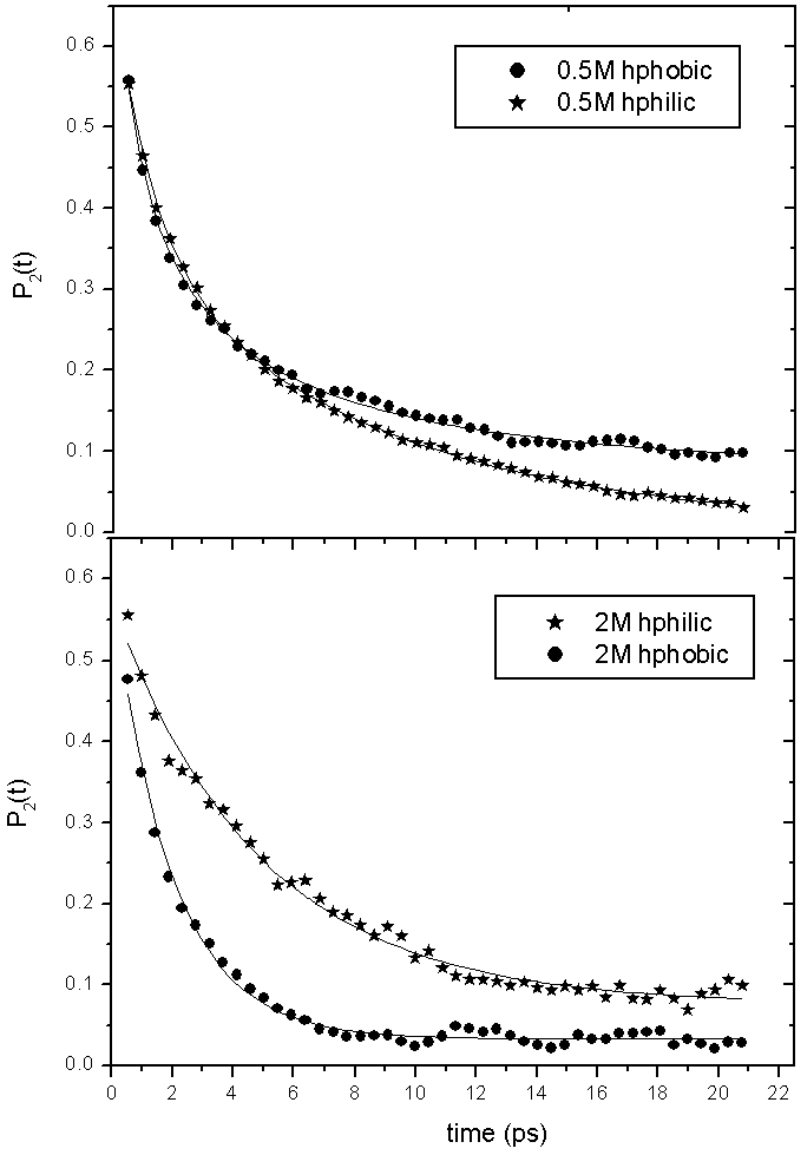

Figure 8. Russo et al.

(a)

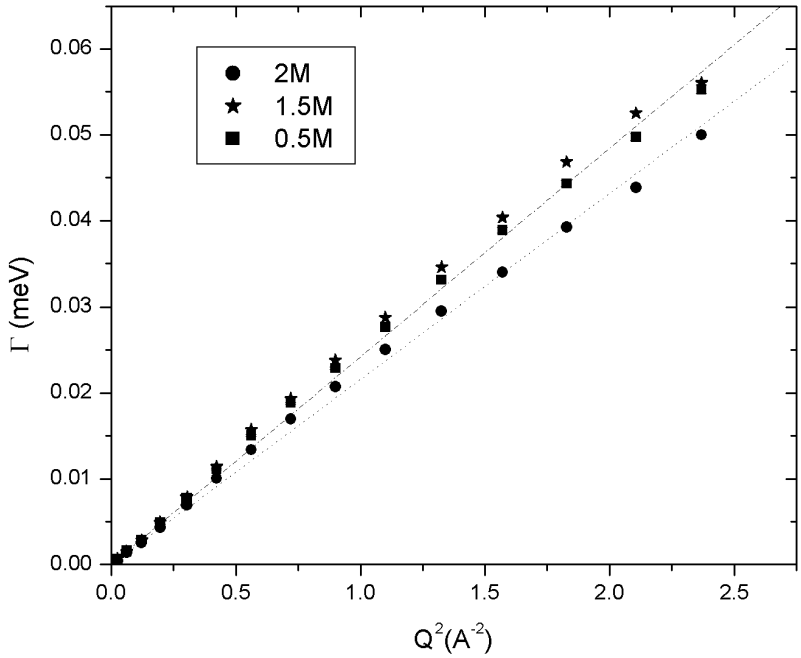

(b)

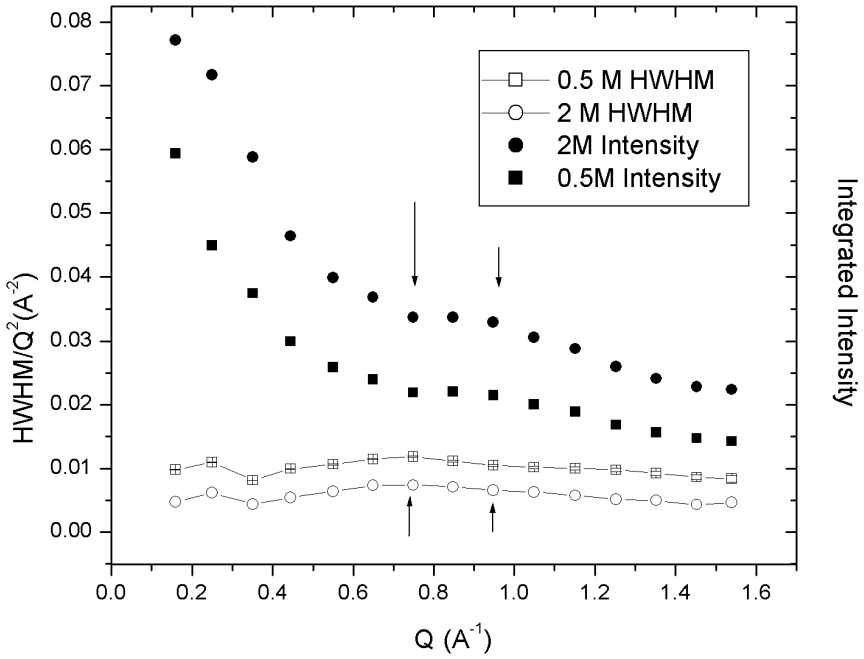

Figure 9. Russo et al.

(c)

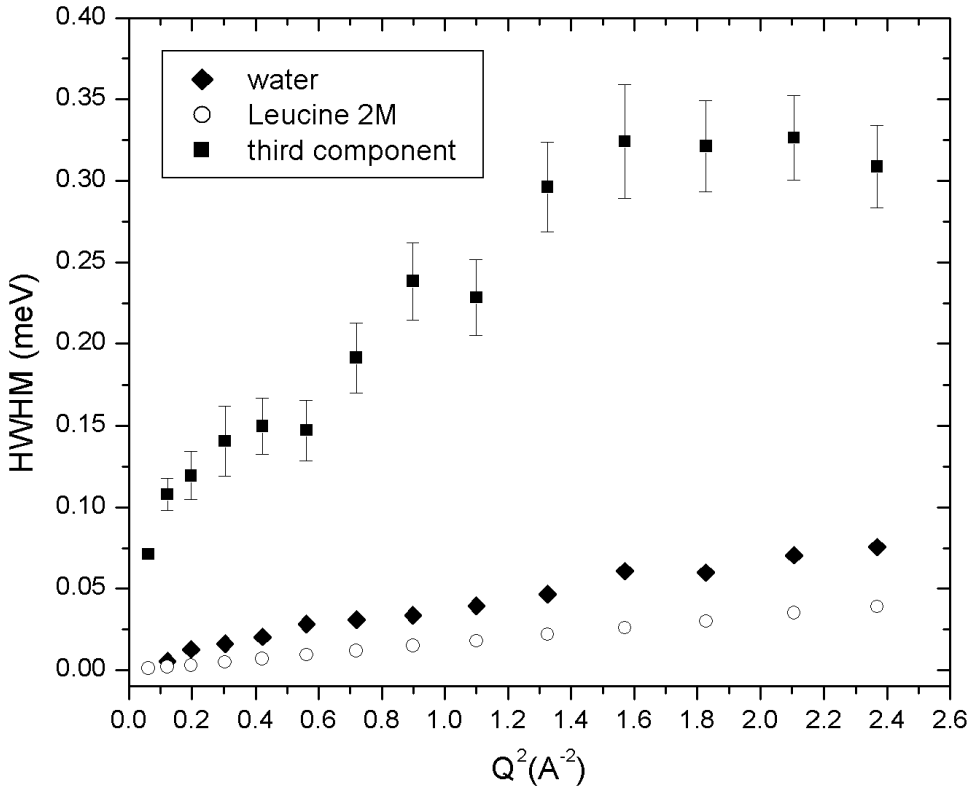

Figure 9. Russo et al.